

# Thermal annealing of roll-cast triblock copolymer films

Ramon J. Albalak and Edwin L. Thomas\*

Department of Materials Science and Engineering, Massachusetts Institute of Technology, Cambridge, MA 02139, USA

and Malcolm S. Capel

National Synchrotron Light Source, Brookhaven National Laboratory, Upton, NY 11973, USA

(Received 19 April 1996)

Polystyrene–polybutadiene–polystyrene triblock copolymers were roll-cast from toluene solutions to form globally oriented films. Microstructural changes following thermal annealing of films with cylindrical and lamellar morphology were monitored using two-dimensional small angle X-ray scattering, transmission electron microscopy and thermomechanical analysis. The microdomains in the unannealed films of cylindrical morphology were found to be assembled on a distorted hexagonal lattice, due to the roll-casting flow field. Thermal annealing significantly improved the alignment and packing of the cylinders, increased grain size, reduced the number of morphological defects and resulted in a 12% decrease in the area per junction. The microstructure of the unannealed films of lamellar morphology was observed to be composed of many small grains with low-angle helicoid surface twist boundaries. Annealing significantly reduced the number of grains and twist boundaries and resulted in a 7% decrease in the area per junction. Molecular models are presented for the relaxation of the chains during the annealing process in both cylindrical and lamellar morphologies based upon 2-D SAXS data and thermomechanical analysis. © 1997 Elsevier Science Ltd.

(Keywords: block copolymers; roll-casting; annealing)

## INTRODUCTION

The preparation and study of oriented block copolymers was originally reported in the early 1970s<sup>1,2</sup> and has recently been the focus of numerous studies<sup>3–13</sup>. These studies have reported on the global orientation of block copolymer films of cylindrical and lamellar morphology using various techniques, both in a molten state and in solution. In the majority of studies, block copolymers with high molecular weights have been processed as a microphase separated melt, due to the inaccessibility of the order–disorder temperature (ODT) without degradation.

This paper focuses on the thermal annealing of triblock copolymer films that were prepared by roll-casting. In this method, a block copolymer solution is processed between rotating cylinders while at the same time the solvent is evaporated at a controlled rate<sup>6,10,11</sup>. As the solvent evaporates, the polymer concentration increases, and the block copolymer microphase separates into globally oriented structures. Depending on the composition of the block copolymers used, the roll-cast films in this study consisted of uniaxial cylindrical polystyrene microdomains assembled on a hexagonal lattice in a polybutadiene matrix, or of unidirectional lamellar domains of polystyrene and polybutadiene.

Previously, we have used one-dimensional small angle X-ray scattering (SAXS)<sup>6,11</sup>, caliper measurements<sup>6</sup> and

thermomechanical analysis<sup>11</sup> to monitor both the microscopic and macroscopic changes that reflect the changes in the microstructure of roll-cast films during annealing. These studies indicated that roll-casting causes the block copolymer molecules to stretch out in the direction of the flow field, and that subsequent annealing allows the molecules to rearrange in less stressed conformations. The present study complements our previous findings by recording two-dimensional SAXS patterns while conducting simultaneous *in situ* annealing experiments and by using TEM to compare the microstructure of unannealed and annealed films. Thermomechanical analysis is employed to monitor the dimensional changes in films of lamellar morphology (thermomechanical analysis of roll-cast films of cylindrical morphology is described elsewhere<sup>11</sup>).

## EXPERIMENTAL

Films of polystyrene–polybutadiene–polystyrene triblock copolymers were cast from toluene solutions containing 40 wt% polymer, using the roll-casting technique previously described<sup>6,10,11</sup>. Films were prepared from two commercial block copolymers manufactured by Dexco Polymers (Houston, TX). The first material used was Vector grade 8550-D, in which the molecular weight of each of the polystyrene end blocks was 10 700, and that of the polybutadiene middle block was 52 000 (J. A. DePoy,

\* To whom correspondence should be addressed

personal communication). Vector 8550-D contains 28 wt% polystyrene so that upon microphase separation from a neutral solvent polystyrene cylinders form in a polybutadiene matrix. The other material employed was Vector grade 4461-D, in which the molecular weight of each of the polystyrene end blocks was 18 500, and that of the polybutadiene middle block was 45 000 (D. A. Reusche and R. L. Lescanec, unpublished results). Vector 4461-D contains 45 wt% polystyrene and microphase separates to form alternating lamellae of polystyrene and polybutadiene.

Roll-cast films were dried in a vacuum oven at 50°C for 48 h in order to remove all traces of the solvent. Films receiving only this post-casting treatment are referred to as 'unannealed' in this paper. Some of the films were then annealed for an additional 96 h under vacuum at 120°C, above the glass-transition temperature of the polystyrene segments of the block copolymer. These films are referred to as 'annealed'.

The effects of thermal annealing of the roll-cast films were studied using small angle X-ray scattering at the National Synchrotron Light Source (Brookhaven National Laboratory). Experiments were performed at a wavelength of  $\lambda = 1.54 \text{ \AA}$  on the Time-Resolved Diffraction Facility (station X12B) using a custom-built two-dimensional gas delay-line detector ( $10 \times 10 \text{ cm}^2$ ,  $512 \times 512$  pixels), interfaced to a real-time histogramming memory system<sup>14</sup>.

*In situ* thermal annealing was performed by heating unannealed roll-cast films, while in the X-ray beam, using a temperature-controlled sample holder equipped with an i.r. heater. The temperature of the films was increased at a rate of approximately  $5^\circ\text{C min}^{-1}$  in increments of  $10^\circ\text{C}$ . The films were maintained at a constant temperature between successive heating ramps to allow 2-D SAXS patterns to be recorded. Patterns were recorded for 30 s at each temperature interval, during which the temperature was maintained constant within  $\pm 1^\circ\text{C}$  of the set point. The initial temperature of the films was  $25^\circ\text{C}$  and the temperature at the end of the heating cycle was  $125^\circ\text{C}$ . The films were then cooled back to  $25^\circ\text{C}$ , during which 2-D SAXS patterns were again recorded at  $10^\circ\text{C}$  increments. For comparison, similar *in situ* heating and cooling experiments were also conducted on annealed roll-cast films.

Transmission electron microscopy (TEM) was performed on the unannealed and annealed roll-cast films using a JEOL 200CX microscope at 200 kV. Thin sections for TEM were prepared using a Reichert-Jung FC 4E cryomicrotome at  $-120^\circ\text{C}$ , and were subsequently stained with osmium tetroxide.

## RESULTS AND DISCUSSION

### Cylindrical morphology

Figure 1a shows a schematic representation of the first few reflections in reciprocal space of the small angle X-ray scattering pattern of an ideal hexagonal lattice, which is schematically pictured in Figure 1b. The two scattering vectors,  $Q_{(01\bar{1}0)}$  and  $Q_{(\bar{2}110)}$ , indicated in Figure 1a correspond to the real space *d*-spacing  $D_{(01\bar{1}0)}$  and  $D_{(\bar{2}110)}$ , shown in Figure 1b. For the purpose of the analysis of the hexagonal structures of roll-cast films of cylindrical morphology, these *d*-spacings will be referred to in this paper as  $D_1$  and  $D_2$ , respectively. For an ideal hexagonal lattice  $D_1/D_2 = \sqrt{3}$ .

In all of the SAXS experiments conducted, the path of the X-ray beam was oriented parallel to the direction of the flow field created during roll-casting (i.e. tangential to the rolls). We refer here to a coordinate system which is consistent with our previous publications on roll-casting<sup>6,10,11</sup> in which this direction is termed *x*, the direction normal to the film surface is termed *y*, and the third (neutral) direction is termed *z*.

Figure 2a shows a two-dimensional small angle X-ray scattering pattern of an unannealed roll-cast film of cylindrical morphology. Comparing Figure 2a to the schematic pattern in Figure 1a, and noting the orientation of the film in the beam as shown by the *y* and *z* axes shown in Figure 1b, indicates that the (0110) planes of the hexagonal lattice are parallel to the surface of the film (i.e. the *xz* plane). This was found to be true for all roll-cast films of cylindrical morphology studied.

The pattern in Figure 2a does not represent a perfect hexagonal lattice. This can be seen, for example, by the fact that the (0110) and the (0 $\bar{1}$ 10) reflections are further away from the origin than the other four first order reflections. This distortion corresponds in real space to a ratio of  $D_1/D_2$  smaller than  $\sqrt{3}$  (i.e. the horizontal (0110) planes are closer to each other than they appear in Figure 1b. Transmission electron microscopy of the unannealed roll-cast films of cylindrical morphology at zero tilt (i.e.  $e^-$  beam along the [0001] direction) also indicates this distortion of the hexagonal lattice (Figure 3).

An unannealed roll-cast film was heated from 25 to  $125^\circ\text{C}$ , and 2-D SAXS patterns were recorded at  $10^\circ\text{C}$  increments. The ratio  $D_1/D_2$  for each pattern is plotted as a function of temperature in Figure 4a, in which the first point ( $25^\circ\text{C}$ ) corresponds to the distorted pattern shown in Figure 2a. As the film is heated, the ratio  $D_1/D_2$  is seen to change gradually from its initial value of 1.51 at  $25^\circ\text{C}$  to 1.74 at  $105^\circ\text{C}$ . Further heating to  $125^\circ\text{C}$  does not bring about additional changes in this ratio, which levels out at a value very close to that for a perfect hexagonal lattice ( $\sqrt{3} \approx 1.73$ ). The overall effects of thermal annealing on the microstructure of the roll-cast films can be seen from comparison of the distorted hexagonal pattern of Figure 2a to the more symmetric 2-D SAXS pattern recorded at  $125^\circ\text{C}$ , shown in Figure 2b. The reflections in Figure 2b are narrower than the corresponding reflections in Figure 2a in both the radial and tangential directions, indicating the improvement in the order of the sample.

Figure 4b presents the value of the ratio  $D_1/D_2$  as a function of temperature during subsequent cooling of the film. The ratio mildly fluctuates within the experimental error and essentially maintains the equilibrium value of  $\sqrt{3}$ . The 2-D SAXS patterns recorded throughout cooling were similar to the pattern recorded at  $125^\circ\text{C}$  (Figure 2b).

*In situ* heating and cooling experiments conducted on annealed roll-cast also showed essentially a constant value of  $D_1/D_2 = \sqrt{3}$  during both heating and cooling of the films. The appearance of the 2-D SAXS patterns recorded throughout these experiments was also comparable to that of the pattern in Figure 2b.

The anisotropic rearrangement of cylinder packing in the *yz* plane of roll-cast films following temperature annealing was originally studied indirectly on a macroscopic scale using thermomechanical analysis (t.m.a.) to monitor the direction-dependent thermal expansion of these films<sup>11</sup>. It was observed that annealing resulted in significant irreversible expansion (+16%) of the films in the *y* direction, accompanied by significant irreversible

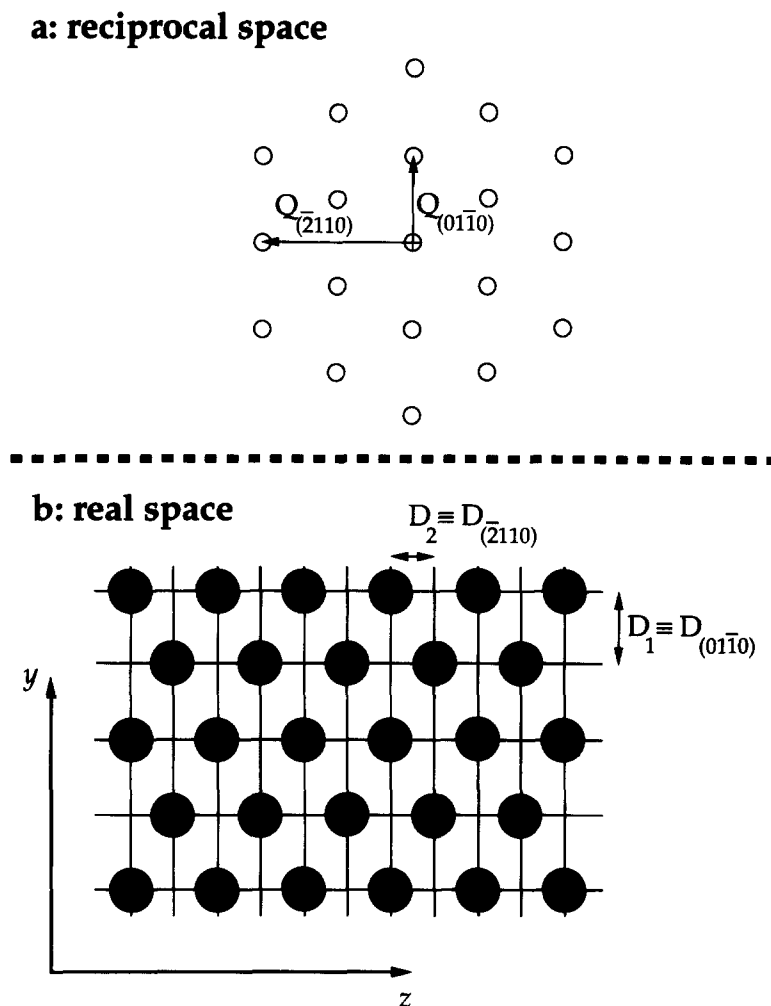


**Figure 1** A schematic representation of the first few reflections in reciprocal space (a) of the small angle X-ray scattering pattern of an ideal hexagonal lattice (b). The two scattering vectors,  $Q_{(0110)}$  and  $Q_{(2110)}$ , indicated in (a) correspond to the real space  $d$ -spacings  $D_{(0110)}$  and  $D_{(2110)}$ , shown in (b). These  $d$ -spacings are referred to  $D_1$  and  $D_2$ , respectively

contraction ( $-17\%$ ) in the  $x$  direction with very little dimensional changes ( $+2\%$ ) in the  $z$  direction. The results of that study combined with our present results indicate the simultaneous microscopic changes in cylinder packing and macroscopic changes in sample dimensions shown schematically in *Figure 5*. Annealing the films allows the polymer molecules, which are stretched in the  $x$  direction (mainly in the  $xy$  plane) during roll casting, to reconfigure into a less stressed structure. This results in shortening of the polystyrene cylinders, which is accompanied by an increase in cylinder diameter and in the value of  $D_1$ . A much smaller increase is also observed in the value of  $D_2$ , as shown in *Figure 6* which presents plots of  $D_1$  and  $D_2$  as a function of temperature during thermal annealing.

The results of the present study, using 2-D SAXS, quantitatively agree reasonably well with those of ref. 11, using thermomechanical analysis. Upon heating from 25 to  $125^\circ\text{C}$ ,  $D_1$  was found by SAXS to increase by about 20%, compared to an expansion of 16% observed in the  $y$  direction using t.m.a.  $D_2$  was found to increase by about 5%, compared to an expansion of 2% observed in the  $z$  direction. The most probable reason for these discrepancies is a certain amount of penetration of the t.m.a. probe into the polymer at temperatures above the  $T_g$  of both blocks. The area per junction,  $\sigma_j$ , for the films of cylindrical morphology may be calculated using the

following equation:

$$\sigma_j = \frac{2M_{\text{PS}}}{R_{\text{cyl}}\rho_{\text{PS}}N_{\text{av}}} \quad (1)$$

in which  $M_{\text{PS}}$  is the molecular weight of the polystyrene block,  $\rho_{\text{PS}}$  is the density of the polystyrene phase,  $N_{\text{av}}$  is Avogadro's number, and  $R_{\text{cyl}}$  is the radius of the polystyrene cylindrical microdomains which is given by:

$$R_{\text{cyl}} = \sqrt{\frac{2D_1 D_2 \phi_{\text{PS}}}{\pi}} \quad (2)$$

in which  $\phi_{\text{PS}}$  is the volume fraction of the polystyrene (equal to 0.25).

Using equation (2), the cylinder radius is calculated to be  $71 \pm 1 \text{ \AA}$  before annealing, and  $81 \pm 1 \text{ \AA}$  after annealing. These calculations assume that the cross section of the polystyrene domains is approximately circular both before and after annealing. Substituting these values into equation (1) indicates that the area per junction decreases during annealing by 12% from  $481 \pm 6 \text{ \AA}^2$  to  $422 \pm 5 \text{ \AA}^2$ .

#### Lamellar morphology

*Figure 7a* shows a two-dimensional small angle X-ray scattering pattern of an unannealed roll-cast film of

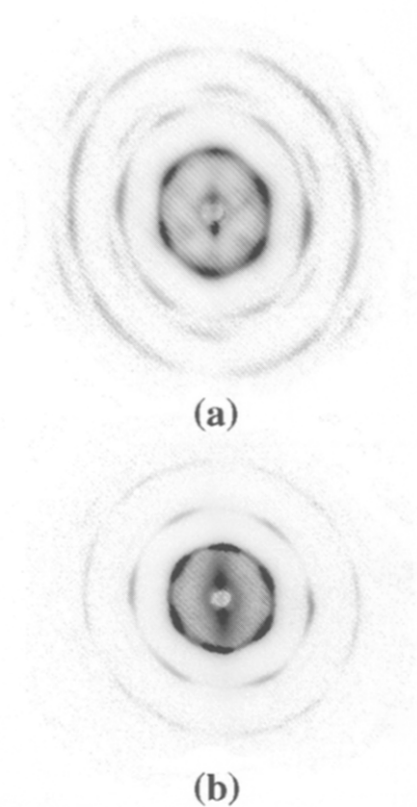


**Figure 2** (a) A two dimensional small angle X-ray scattering pattern of an unannealed roll-cast film of cylindrical morphology, with the X-ray beam normal to the  $yz$  plane (i.e. along  $x$ ) of the film. The pattern does not represent a perfect hexagonal lattice. This can be seen, for example, by the fact that the  $01\bar{1}0$  and the  $0\bar{1}10$  reflections are further away from the origin than the other four first order reflections. (b) A two-dimensional small angle X-ray scattering pattern of the same film recorded at  $125^\circ\text{C}$ , exhibiting improved order

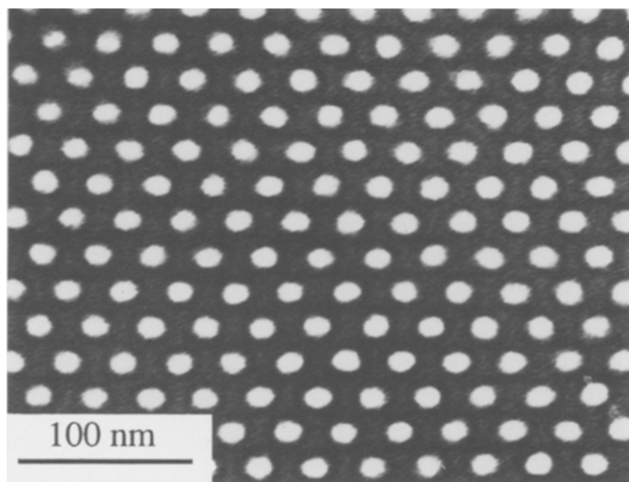


**Figure 3** Transmission electron microscopy of the unannealed roll-cast films of cylindrical morphology at zero tilt indicating the distortion of the hexagonal lattice

lamellar morphology. The reflections in *Figure 7a* indicate that the lamellae lie in the  $xy$  plane, as shown schematically in *Figure 8*, which represents the orientation of the lamellae in all the vector 4461-D samples used in this study. We note that in previous work<sup>6</sup>, block copolymer films have been roll-cast under conditions which cause the lamellae to lie in the  $xz$  plane. The

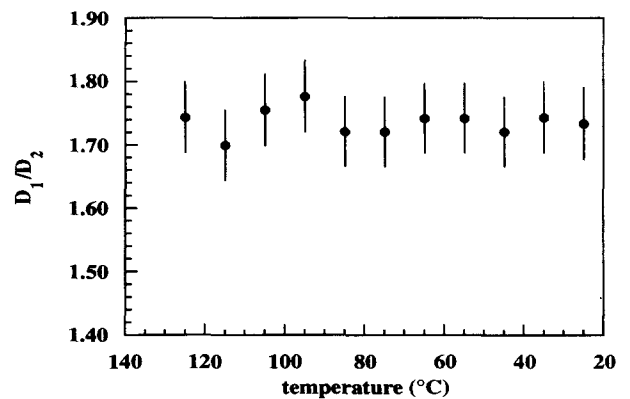
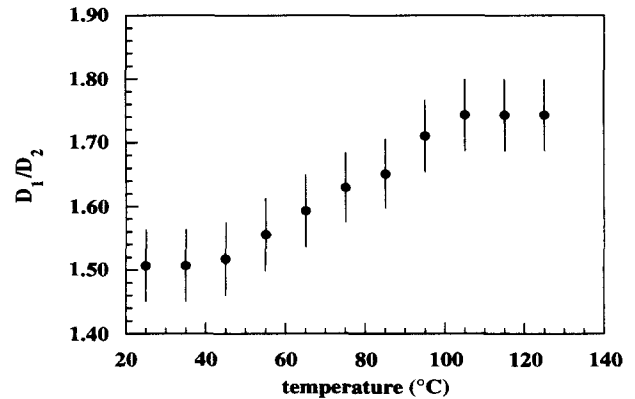


**Figure 4** (a) A plot of the ratio  $D_1/D_2$  as a function of temperature during thermal annealing of a roll-cast film with cylindrical morphology. As the film is heated, the ratio  $D_1/D_2$  increases and levels out at about  $\sqrt{3}$ , which corresponds to a perfect hexagonal lattice. (b) A plot of the ratio  $D_1/D_2$  as a function of temperature during subsequent cooling of the film after heating to  $125^\circ\text{C}$ . As the film is cooled, the ratio  $D_1/D_2$  maintains its value of approximately  $\sqrt{3}$

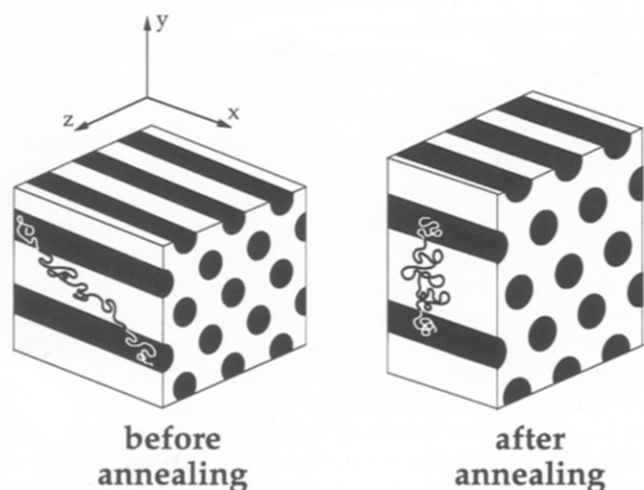


**Figure 5** A schematic representation of the simultaneous microscopic changes in cylinder packing and macroscopic changes in sample dimensions during annealing. The polymer molecules, which are stretched in the  $x$  direction (mainly in the  $xy$  plane) during roll casting, reconfigure into a less stressed structure. This results in shortening of the polystyrene cylinders, which is accompanied by an increase in cylinder diameter and in the value of  $D_1$

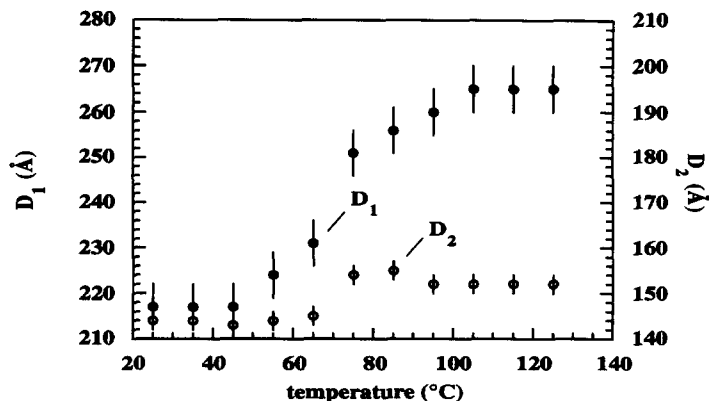


**Figure 6** A plot of the  $d$ -spacings  $D_1$  and  $D_2$  as a function of temperature during thermal annealing of a roll-cast film with cylindrical morphology. The changes in  $D_1$  are larger than those in  $D_2$

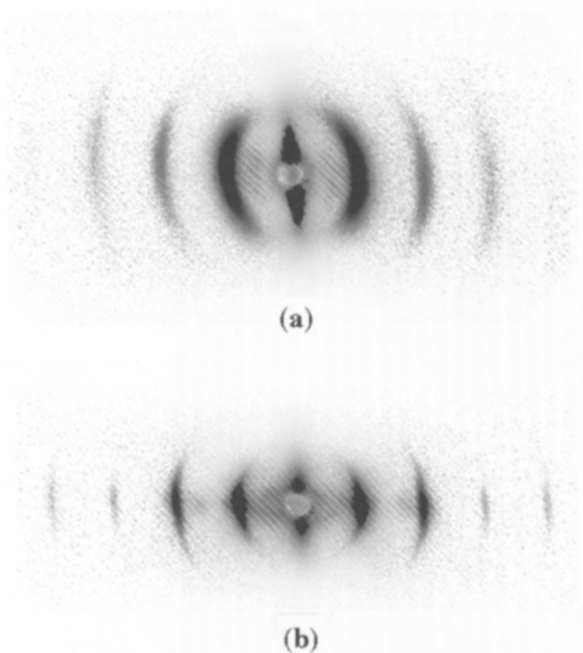


**Figure 7** (a) A two-dimensional small angle X-ray scattering pattern of an unannealed roll-cast film of lamellar morphology, with the X-ray beam normal to the  $yz$  plane (i.e. along  $x$ ) of the film. The broadening of the reflections is due to the presence of numerous grains which are slightly misaligned. (b) A two-dimensional small angle X-ray scattering pattern of the film recorded at 125°C. The reflections are sharper and more intense than the reflections of the unannealed film in (a)

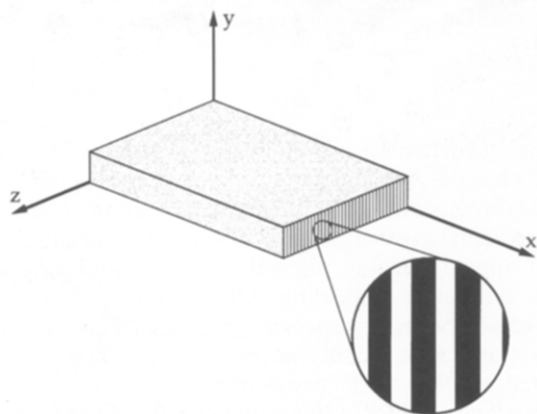


**Figure 8** A schematic representation of the orientation of the lamellae, which lie in the  $xy$  plane of the roll-cast films

dependence of the directional orientation of the lamellae on processing conditions has also been observed by others<sup>4,9,13</sup>.

Figure 9 is a transmission electron micrograph viewing normal to the  $yz$  plane (i.e. along  $x$ ) of an unannealed roll-cast film of lamellar morphology. The general unidirectional orientation of the lamellae is clearly evident. However, the structure is composed of many small grains with numerous helicoid surface twist boundaries which result in the azimuthal broadening of the reflections seen in Figure 7a. Helicoid surface twist grain boundaries have been observed to form at relatively low twist angles of up to 15°<sup>15</sup>.

In an experiment similar to that conducted with films of cylindrical morphology, an unannealed roll-cast film of lamellar morphology was heated from 25 to 125°C, and 2-D SAXS patterns were recorded at 10°C increments. The  $d$ -spacing ' $D$ ' corresponding to the first reflection in each pattern is plotted as a function of temperature in Figure 10a in which the first point (25°C) corresponds to the pattern shown in Figure 7a. As the film is heated, the value of  $D$  changes from its initial value around 250 Å to about 270 Å at temperatures of 75°C and above. The 2-D SAXS pattern recorded at 125°C (Figure 7b) exhibits much sharper and intense reflections than those of the unannealed film in Figure 7a.

Figure 10b presents the value of  $D$  as a function of temperature during subsequent cooling of the film. As with the films of cylindrical morphology, the cooling of the annealed film has little effect on the  $d$ -spacing, which essentially maintains a value of 270 Å as the temperature is decreased. The 2-D SAXS patterns recorded throughout cooling were similar to Figure 7b. The effect of thermal annealing on the morphology of these films is clearly demonstrated by comparing TEM images before (Figure 9a) and after annealing (Figure 9b); the number of grains and twist boundaries has significantly diminished and the overall structure approaches that of a 'single-crystal'.

*In situ* heating and cooling experiments conducted on annealed roll-cast films of lamellar morphology also showed essentially a constant value of  $D = 270$  Å during both heating and cooling of the films. The appearance of the 2-D SAXS patterns recorded throughout these experiments was comparable to that of the pattern in Figure 7b.

Thermomechanical analysis was performed on unannealed films of lamellar morphology using a Perkin Elmer TMA 7. The changes in film dimensions were measured

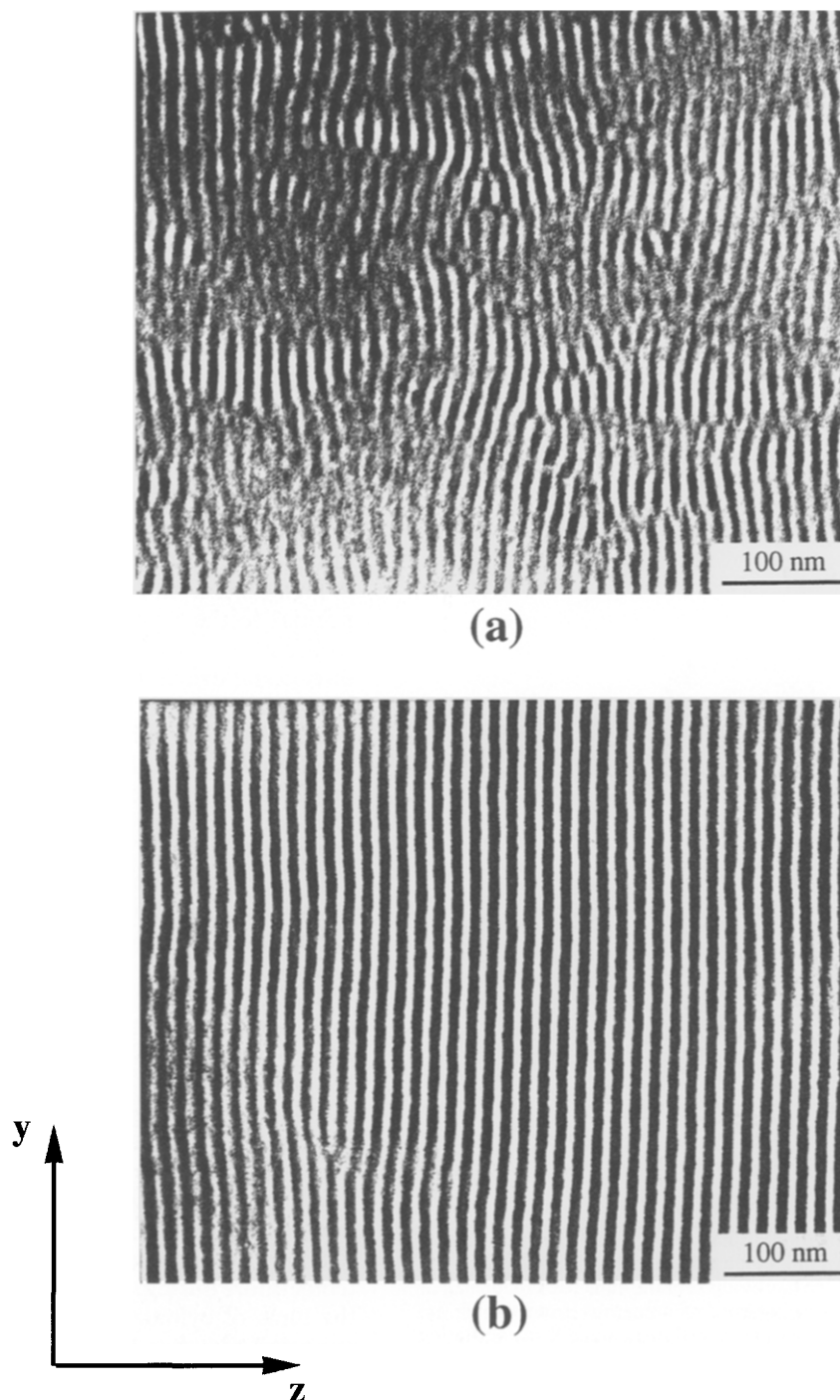


**Figure 9** (a) A transmission electron micrograph of a  $yz$  plane of an unannealed roll-cast film of lamellar morphology. The structure is composed of many small grains with numerous helicoid surface twist boundaries. (b) A transmission electron micrograph of a  $yz$  plane of an annealed roll-cast film of lamellar morphology. The number of grains and twist boundaries has diminished

in the  $x$ ,  $y$  and  $z$  directions as a function of heating from 25 to 125°C at a rate of 10°C min<sup>-1</sup>, maintaining the films isothermally at 125°C for 10 min and subsequently cooling the films back to 25°C at a rate of 10°C min<sup>-1</sup>. The films were found to irreversibly expand by 18% in the  $y$  direction and by 7% in the  $z$  direction, and to contract simultaneously and irreversibly by 25% in the  $x$  direction. The expansion by 7% observed in the  $z$  direction agrees with the 8% increase in the  $d$ -spacing measured by SAXS. Due to the lack of periodicity in the  $x$  and  $y$  directions, the t.m.a. results in these directions cannot be compared with SAXS data.

*Figure 11* schematically shows the simultaneous microscopic changes in  $d$ -spacing and macroscopic changes in sample dimensions due to thermal annealing. The figure also presents a schematic of a typical molecule, as it would appear viewing normal to the  $xz$  and  $yz$  planes before and after annealing. Our results indicate that prior to annealing, the polymer molecules are stretched in the  $x$  direction, mainly in the  $xz$  plane. The molecule depicted has very little 'projection' in the  $y$  direction, as shown schematically in the  $yz$  plane view of the molecule before annealing. Annealing the polymer allows the molecule to reconfigure into a less stressed structure,

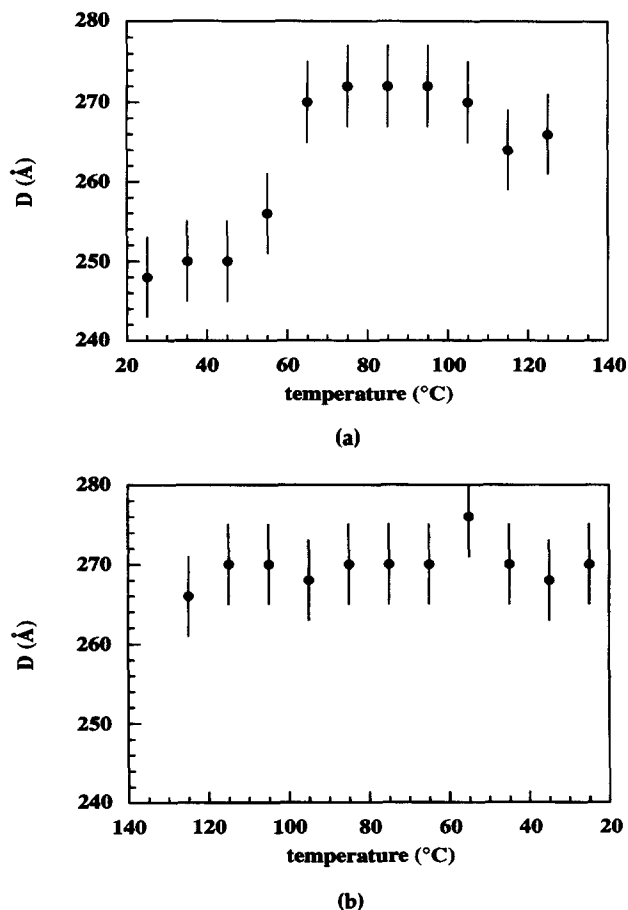


**Figure 10** (a) A plot of the lamellar  $d$ -spacing,  $D$ , as a function of temperature during thermal annealing of a roll-cast film with lamellar morphology. (b) A plot of the lamellar  $d$ -spacing,  $D$ , as a function of temperature during subsequent cooling of the film after heating to 125°C. As the film is cooled, the  $d$ -spacing maintains its value of approximately 270 Å

which is now similar if viewed along the  $x$  axis or the  $y$  axis (right illustration). However, although the projections of the molecule are now similar in both the  $xz$  and  $yz$  planes, the change in the projection of the molecule in the  $y$  direction (in the  $yz$  plane) relative to the unannealed state is larger than the change in its projection in the  $z$  direction (in the  $xz$  plane). Hence the expansion in the  $y$  direction (+18%) is larger than the expansion in the  $z$  direction (+7%). The sum of these expansions is equal to the contraction in the  $x$  direction (−25%), indicating, as expected, that there is no overall change in sample volume upon annealing.

The area per junction may also be calculated for the films of lamellar morphology using the following relation:

$$\sigma_j = \frac{2M_{PS}}{D\phi_{PS}\rho_{PS}N_{av}} \quad (3)$$

The calculated area per junction before annealing is  $576 \pm 12 \text{ \AA}^2$ . After annealing this decreases by 7% to  $534 \pm 10 \text{ \AA}^2$ .

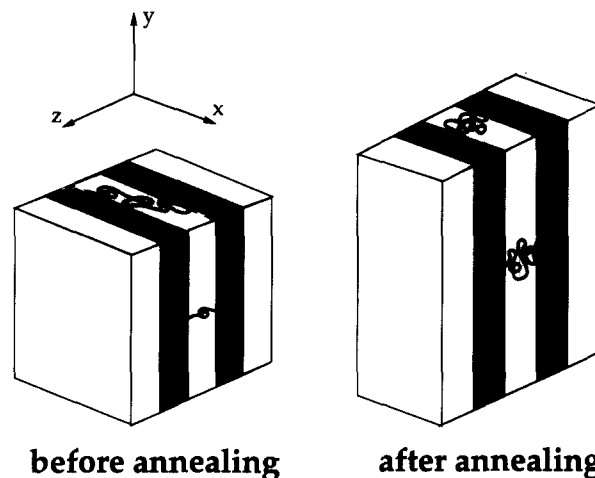


**Figure 11** A schematic showing the simultaneous microscopic changes in  $d$ -spacing and the macroscopic changes in sample dimensions due to thermal annealing. The figure also presents a schematic of a typical molecule, as it would appear viewing normal to the  $xz$  and  $yz$  planes before and after annealing. Note: in each of the two illustrations representing the structure before and after annealing, two projections of the same molecule are shown, and not two different molecules

#### ACKNOWLEDGEMENTS

This research was supported by Master Builders, Inc. We gratefully acknowledge Dexco Polymers for supplying the triblock copolymers used. Work at Brookhaven National Laboratory was supported by DOE.

#### REFERENCES

- Keller, A., Pedemonte, E. and Willmouth, F. M., *Colloid Polym. Sci.* 1970, **238**, 385.
- Le Meur, J. Terrisse, J., Schwab, C. and Goldzene, *J. Phys. (Paris), Colloq.* 1971, **5**, 301.
- Morrison, F. A., Winter, H. H., Gronski, W. and Barnes, J. D., *Macromolecules* 1990, **23**, 4200.
- Koppi, K. A., Tirrell, M., Bates, F. S., Almdal, K. and Colby, R. H., *J. Phys. II Fr.* 1992, **2**, 1941.
- Almdal, K., Koppi, K. A., Bates, F. S. and Mortensen, K., *Macromolecules* 1992, **25**, 1743.
- Albalak, R. J. and Thomas, E. L., *J. Polym. Sci., Polym. Phys. Ed.* 1993, **31**, 37.
- Morrison, F. A., Mays, J. W., Muthukumar, M., Nakatani, A. I. and Han, C. C., *Macromolecules* 1993, **26**, 5271.
- Koppi, K. A., Tirrell, M. and Bates, F. S., *Phys. Rev. Lett.* 1993, **70**, 1449.
- Winey, K. I., Patel, S. S., Larson, R. G. and Watanabe, H., *Macromolecules* 1993, **26**, 4373.
- Albalak, R. J. and Thomas, E. L., *J. Polym. Sci., Polym. Phys. Ed.* 1994, **32**, 341.
- Albalak, R. J., *Polymer* 1994, **35**, 4115.
- Okamoto, S., Saijo, K. and Hashimoto, T., *Macromolecules* 1994, **27**, 5547.
- Zhang, Y., Wiesner, U. and Spiess, H. W., *Macromolecules* 1995, **28**, 778.
- Capel, M. S., Smith, G. C. and Yu, B., *Rev. Sci. Instrum.* 1995, **66**, 2295.
- Gido, S. P., Gunther, J., Thomas, E. L. and Hoffman, D., *Macromolecules*, 1993, **26**, 4506.